Fast Dissolving Curcumin Cocrystals

ARTICLE *in* CRYSTAL GROWTH & DESIGN · AUGUST 2011

Impact Factor: 4.89 · DOI: 10.1021/cg200704s

4 AUTHORS:

Palash Sanphui
Indian Institute of Science
26 PUBLICATIONS **514** CITATIONS
SEE PROFILE

Rajesh Goud Nagula
University of Michigan
19 PUBLICATIONS **383** CITATIONS
SEE PROFILE

U B Rao Khandavilli
University College Cork
11 PUBLICATIONS **121** CITATIONS
SEE PROFILE

Ashwini Nangia
University of Hyderabad
273 PUBLICATIONS **7,121** CITATIONS
SEE PROFILE

CRYSTAL GROWTH & DESIGN

ARTICLE

pubs.acs.org/crystal

Fast Dissolving Curcumin Cocrystals

Palash Sanphui,[†] N. Rajesh Goud,[†] U. B. Rao Khandavilli,[‡] and Ashwini Nangia*[,†,‡]

[†]School of Chemistry and [‡]Technology Business Incubator, University of Hyderabad, Prof. C. R. Rao Road, Gachibowli, Central University P.O., Hyderabad 500046, AP, India

Supporting Information

ABSTRACT: Curcumin is the principal curcuminoid of the popular Indian spice turmeric. Despite the diverse pharmacological activities of this bioactive phenol, its application as a drug is severely limited by poor aqueous solubility. We report novel cocrystals of curcumin (**1**) with resorcinol and pyrogallol obtained by liquid-assisted grinding. Curcumin−resorcinol (**1a**) (1:1) and curcumin−pyrogallol (**1b**) (1:1) were characterized by X-ray diffraction, thermal analysis, FT-IR, FT-Raman, and solid-state ^{13}C NMR spectroscopy. The 1:1 cocrystal stoichiometry is sustained by O−H···O hydrogen bonds between the phenolic OH groups of the coformers to the carbonyl group of curcumin. The melting point of the cocrystals is in between that of curcumin and the coformer and the lower melting cocrystal **1b** is more soluble than higher melting **1a**. The dissolution rates of curcumin−resorcinol (**1a**) and curcumin−pyrogallol (**1b**) in 40% EtOH−water are ∼5 and ∼12 times faster than that for curcumin.

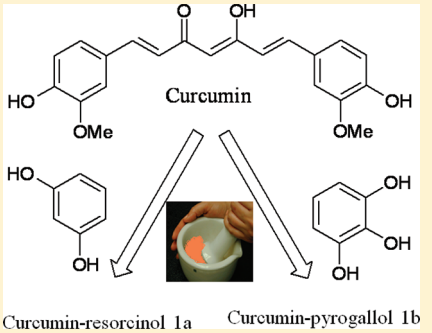

INTRODUCTION

Active pharmaceutical ingredients (API) with poor physicochemical properties, notably solubility and stability, pose a serious threat to clinical development because of late-stage failure of drug candidates.[1] A cocrystal[2] may be defined as a multicomponent molecular complex in a definite stoichiometric ratio of solids that interact through noncovalent interactions, predominantly hydrogen bonds. In pharmaceutical cocrystals,[3] one of the components is an investigational or marketed drug molecule (the active pharmaceutical ingredient or API) and the second component (the coformer) is a safe chemical for human consumption selected from the GRAS list of the US FDA (generally regarded as safe additive chemicals by the Food and Drugs Administration).[4] In recent years, cocrystals have been found to offer an attractive platform to improve the solubility and dissolution rate of pharmaceuticals without compromising on the stability of the solid form. Remenar et al.[5] reported cocrystals of itraconazole with carboxylic acids that exhibited 4−20-fold higher concentration than the insoluble, crystalline drug form. The best examples of 2:1 cocrystals of L-tartaric acid and L-malic acid with itraconazole were able to achieve and sustain dissolution profiles comparable to the marketed amorphous form as Sporanox capsule. The main advantages of cocrystals over the alternate method of amorphous drugs for solubility improvement is that the former adducts being crystalline in nature are relatively stable and less prone to phase transformations. Second, the large number of GRAS coformers makes it possible to explore several cocrystals for the same API.[6] High solubility is a necessary condition for good oral absorption of an active drug[7] to ensure optimal delivery, which is related to issues such as bioavailability, biopharmaceutical classification, biowaivers, and bioequivalence. We report preliminary results on fast dissolving cocrystals of curcumin.

Curcumin (**1**, diferuloylmethane) is the active ingredient in the traditional herbal remedy and dietary Indian spice turmeric; it is derived from the rhizome of the herb *Curcuma longa*.[8,9] Curcumin possesses diverse pharmacological activities, such as anti-inflammatory, antioxidant, antiproliferative, antiangiogenic, and anticancer.[10−13] The molecule exists as keto−enol tautomers (Scheme 1), being present predominantly in the keto form in acidic and neutral solution, whereas the enol tautomer is stable in alkaline medium. Curcumin is safe even at a high doses of 12 g/day[14,15] in animal and human trials, but its effectiveness is limited by low solubility and poor bioavailability in aqueous medium. The poor bioavailability of curcumin is due to its low absorption, rapid metabolism, and fast systemic elimination from the biological system.[16] Curcumin decomposes rapidly in neutral and alkaline medium, >90% decomposition occurs within 30 min in pH 7.4 buffer medium.[17] Hence, despite its efficacy and safety, curcumin is still not approved as a therapeutic agent. The stability and bioavailability of curcumin has been improved by several methods: (1) by adding adjuvants such as piperine to block the metabolic pathways of curcumin; (2) with novel drug delivery platforms such as nanoparticles, liposomes, micelles, and phospholipid complexes; and (3) with concomitant administration of lecithin, quercetin, genistein, eugenol, terpinol, etc. to increase the bioavailability.[16−18] The aqueous solubility of curcumin was enhanced 38-fold in the presence of 1−10% (w/v) rubusoside.[19] The bioavailability of curcumin in water and lipid medium was enhanced by complexation with phosphatidyl choline in equimolar ratio.[20]

The instability of curcumin at physiological pH may be ascribed to the β-diketone linker in the seven carbon chain of curcumin. We reasoned that the reactivity of the keto−enol group could be modified through hydrogen bonding with

Received: June 4, 2011
Revised: July 26, 2011
Published: July 27, 2011

Scheme 1. Chemical Structure of Curcumin 1 (Keto and Enol Tautomers) and Coformers Resorcinol and Pyrogallol

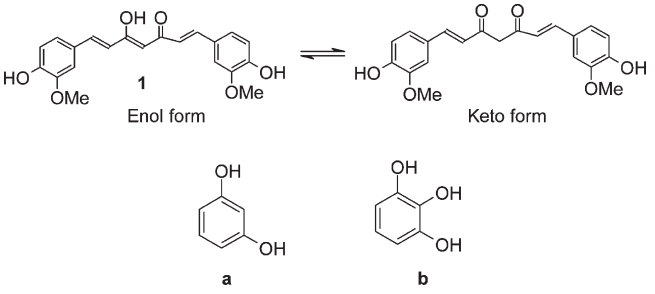

phenolic compounds in cocrystals, which in turn might provide more soluble and stable curcumin solid-state forms. A few examples of pharmaceutical cocrystals involving a phenol API or coformer were reported[21−23] while our work was in progress. Cocrystals can alter the physicochemical properties (e.g., stability, solubility, bioavailability) of drugs in a controlled manner.[24,25] We recently reported novel polymorphs of curcumin that exhibited superior dissolution rate compared to the known crystalline modification.[26] However, the metastable nature of such fast dissolving polymorphs observed in follow-up experiments could pose a serious concern for further development. A solid form screen of curcumin with phenolic coformers[27] afforded novel cocrystals with resorcinol and pyrogallol (Scheme 1). These curcumin cocrystals were characterized by X-ray diffraction, spectroscopy, and thermal techniques. Resorcinol is a safe coformer molecule from the GRAS list,[4] and pyrogallol[28] and its derivatives[29] exhibit anticancer activity.

RESULTS AND DISCUSSIONS

Crystal Structure Analysis. The cocrystallization of curcumin−resorcinol (**1a**) and curcumin−pyrogallol (**1b**) was attempted by solid-state and liquid-assisted grinding methods. The main advantage of solid-state grinding technique is that it overcomes complications due to possible solvent/water inclusion during solution crystallization, but a drawback is that the product is often microcrystalline and hence not suitable for single crystal X-ray diffraction. Addition of a few drops of a solvent as lubricant (here EtOH) to accelerate molecular mobility during grinding/kneading, referred to as liquid-assisted grinding,[30] facilitated quantitative formation of the product cocrystals. Curcumin−resorcinol (**1a**) (1:1) and curcumin−pyrogallol (**1b**) (1:1) cocrystals were obtained by liquid-assisted manual grinding of the individual solid components for 30 min in a mortar pestle after adding 5−6 drops of EtOH. The starting materials were consumed and new peaks observed in the powder X-ray diffraction pattern. Diffraction quality single crystals of **1a** and **1b** were obtained by slow crystallization of the components in 1:1 molar ratio from EtOH−benzene solvent mixture (see Experimental Section). The cocrystal composition and stoichiometry was confirmed from the crystal structure (Table 1) (see Figure S1 in Supporting Information for the ORTEP diagram). Among the 1,3-diketone and β-keto−enol tautomers of curcumin **1**, the keto−enol tautomer is more stable by 6.7 kcal/mol in the gas phase, and this tautomer is present in its crystal structures.[31]

The asymmetric unit of **1a** in the monoclinic space group $P2_1/c$ contains one molecule each of curcumin and resorcinol. The curcumin molecule is almost planar, similar to that present in the metastable polymorphs of curcumin.[26] In contrast, the stable crystalline modification of curcumin has a twisted conformation.[32] The dihedral angle between the least-squares planes passing through C4−C7−C8−C9−C10−C11 and C12−C13−C14 atoms of curcumin is 4.9° in cocrystal **1a** (the values in polymorph **2** and **3** of curcumin are 9.4° and 17.0°, 11.7° respectively). There is an intramolecular hydrogen bond [O4−H4A···O3, 1.79 Å, 2.569(5) Å, 132.9°] in the enol tautomer. Curcumin molecules form an intermolecular O−H···O hydrogen bond [O1−H1···O6, 2.57 Å, 3.506(6) Å, 159.3°] between the phenol O−H donor and OMe acceptor. The resorcinol molecules are inclined at a dihedral angle of 64.9° to curcumin. Two resorcinol molecules donate O−H···O hydrogen bonds along the *a*-axis to the carbonyl group of curcumin [O7−H7A···O3, 1.81 Å, 2.773(6) Å, 165.4°; O8−H8A···O3, 2.09 Å, 2.921(6) Å, 140.4°] (Figure 1a). Weak C−H···O and C−H···π interactions play an auxiliary role in structure stabilization (Figure 1b). Hydrogen bonds are listed in Table 2.

The asymmetric unit of **1b** in the monoclinic space group $P2_1/n$ contains one molecule each of curcumin and pyrogallol. The curcumin molecule is almost planar: the dihedral angle between the least-squares planes in curcumin is 6.7°. There is an intramolecular hydrogen bond [O4−H4A···O3, 1.76 Å, 2.552(5) Å, 135°] in the enol tautomer. Two pyrogallol molecules hydrogen bond along the *a*-axis to the carbonyl oxygen of the β-keto group [O7−H7B···O3, 1.91 Å, 2.748(5) Å, 141°;

Table 1. Crystallographic Data for Curcumin Cocrystals 1a and 1b

curcumin	curcumin−resorcinol (1:1), **1a**	curcumin−pyrogallol (1:1), **1b**
empirical formula	C_{21} H_{20} O_6, C_6 H_6O_2	C_{21} H_{20} O_6, C_6 H_6 O_3
formula weight	478.48	494.48
crystal system	monoclinic	monoclinic
space group	$P2_1/c$	$P2_1/n$
T (K)	298(2)	100(2)
a (Å)	7.7321(9)	7.3706(6)
b (Å)	16.1990(19)	15.8001(10)
c (Å)	19.558(3)	19.8972(14)
α (deg)	90	90
β (deg)	101.095(12)	92.933(7)
γ (deg)	90	90
V (Å^3)	2403.9(5)	2314.1(3)
D_{calcd} (g cm^{-3})	1.322	1.419
μ (mm^{-1})	0.098	0.107
θ range	2.72−20.76	2.77−26.37
Z	4	4
range h	−7 to +7	−9 to +9
range k	−16 to +16	−19 to +19
range l	−19 to +19	−24 to +24
reflections collected	4011	10468
total reflections	2467	4721
observed reflections	1287	2414
R_1 [$I > 2\sigma(I)$]	0.0687	0.0923
wR_2 (all)	0.2029	0.2867
goodness-of-fit	0.983	1.030
diffractometer	Oxford-CCD	Oxford-CCD

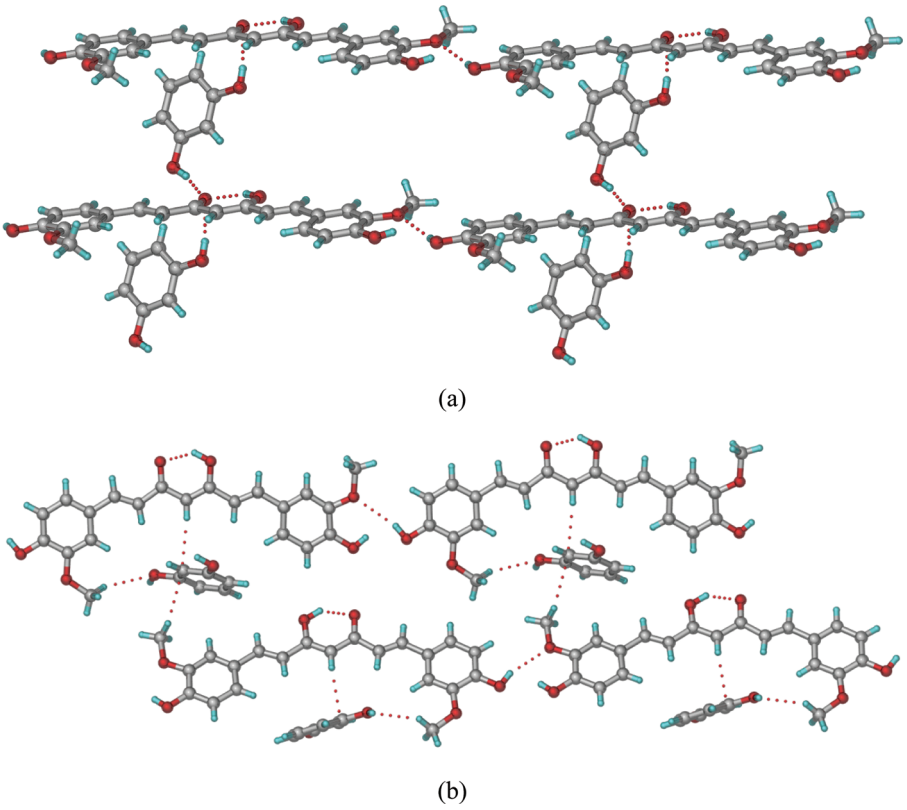

Figure 1. (a) O−H···O hydrogen bond between curcumin and resorcinol molecules along the *a*-axis in cocrystal **1a**. (b) O−H···O, C−H···O, and C−H···π interactions between curcumin and resorcinol molecules in the crystal structure.

Table 2. Hydrogen Bonds in Crystal Structures (Neutron-Normalized Distances)

crystal forms	interaction	H···A/Å	D···A/Å	∠D−H···A/deg	symmetry code
curcumin−resorcinol (**1a**)	O1−H1···O6	2.57	3.506(6)	159	$-1+x, y, -1+z$
	O4−H4A···O3	1.79	2.569(5)	133	intramolecular
	O5−H5A···O1	2.01	2.750(8)	130	$1+x, y, 1+z$
	O5−H5A···O6	2.13	2.648(9)	111	intramolecular
	O7−H7A···O3	1.81	2.773(6)	166	$2-x, 1-y, -z$
	O8−H8A···O3	2.10	2.921(6)	140	$1-x, 1-y, -z$
	C21−H21A···O8	2.68	3.414(6)	133	$x, 1/2-y, 1/2+z$
curcumin−pyrogallol (**1b**)	O1−H1···O2	2.16	2.620(5)	106	intramolecular
	O4−H4A···O3	1.76	2.552(5)	135	intramolecular
	O5−H5A···O1	1.98	2.724(5)	130	$x, y, 1+z$
	O1−H1···O9	1.97	2.814(5)	142	$3/2-x, 1/2+y, 1/2-z$
	O9−H9···O5	1.83	2.681(5)	143	$3/2-x, 1/2+y, 1/2-z$
	O7−H7B···O3	1.91	2.748(5)	141	$-2+x, y, z$
	O8−H8A···O3	1.78	2.665(5)	148	$x, y, -1+z$
	C8−H8···O7	2.66	3.738(6)	171	$1-x, 1-y, -z$
	C20−H20C···O8	2.41	3.366(6)	146	$1-x, 1-y, -z$
	C7−H7···O9	2.41	3.480(6)	168	$x, y, -1+z$
	C23−H23···O9	2.25	3.310(6)	165	$-1+x, y, z$

O8−H8A···O3, 1.78 Å, 2.665(5) Å, 148°]. Curcumin molecules are arranged in infinite chains linked through an intermolecular O−H···O hydrogen bond between the phenolic OH groups of adjacent molecules [O5−H5A···O1, 1.98 Å, 2.724(5) Å, 130°]. An O−H···O hydrogen-bonded trimer [O1−H1···O9, 1.97 Å, 2.814(5) Å, 142°; O9−H9···O5, 1.83 Å, 2.681(5) Å, 143°] between the phenol OH of two curcumin molecules with pyrogallol oxygen acceptor forms a ring motif of $R_3^3(6)$ graph set notation[33] (Figure 2a). A few crystal structures having the O−H···O trimer synthon extracted from the Cambridge Structural Database[34] are HESKOF,[35] QEXXEW,[36] SEFRIE,[37] and XEFSIK[38] (six alphabet CSD REFCODEs).

dx.doi.org/10.1021/cg200704s |*Cryst. Growth Des.* 2011, 11, 4135–4145

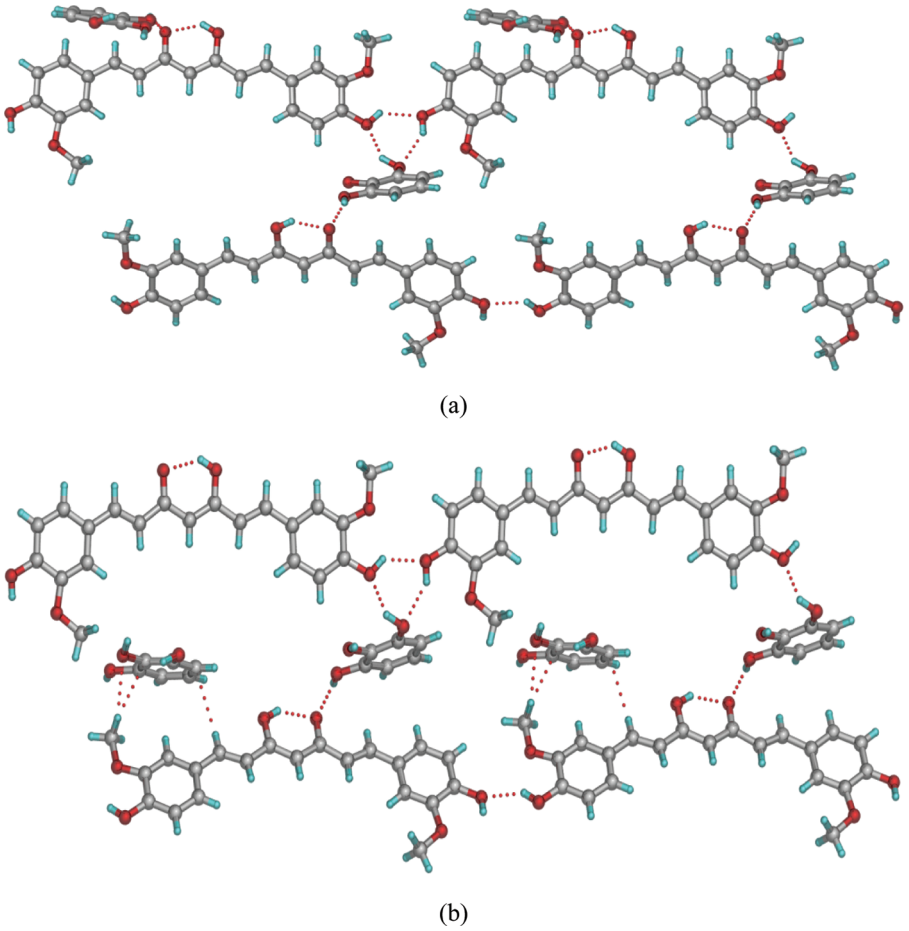

Figure 2. (a) O−H···O trimer between two curcumin and one pyrogallol molecules in cocrystal **1b**. (b) O−H···O, C−H···O, and C−H···π interactions between curcumin and pyrogallol molecules in the crystal structure.

Weak C−H···O and C−H···π interactions stabilize the overall packing of cocrystal structure **1b** (Figure 2b).

The molecular overlay of curcumin in polymorphs **1**−**3**, curcumin−resorcinol **1a**, and curcumin−pyrogallol **1b** displays the almost planar conformation of curcumin molecule in its metastable polymorphs and cocrystals, but the molecule is twisted in the stable modification (Figure 3). The cocrystal of curcumin with resorcinol is a pharmaceutical cocrystal because resorcinol has GRAS status,[4] and curcumin−pyrogallol may be classified as a drug−drug cocrystal,[39−41] given the lung cancer and tumor growth inhibition activity of pyrogallol.[28] Attempts to make cocrystals of curcumin with other phenols such as catechol, orcinol, phloroglucinol, and hydroquinone were unsuccessful.

Thermal Analysis. The thermal stability of curcumin cocrystals **1a** and **1b** was examined by differential scanning calorimetry (DSC) (Figure 4). They exhibited a single endotherm peak at 166 and 158 °C, respectively, indicative of a homogeneous solid phase. The melting point of both cocrystals is in between that of curcumin and the coformer[42] (curcumin, 177 °C; resorcinol, 110 °C; and pyrogallol, 131 °C). The higher onset temperature of cocrystal **1a** compared to **1b** does not correlate with coformer melting point.

Powder X-ray Diffraction. Powder X-ray diffraction is a fingerprint characterization method for solid phases, such as cocrystals and salts.[43,44] If the resulting PXRD of the solid product after grinding the pure solid compounds (the API and the coformer) is different from that of the reactants, then it may be inferred that a new solid phase has formed. The unexpected formation of a new polymorph for one of the components during grinding and/or due to the presence of a coformer as an additive is another possibility.[45] The presence of both the molecular components and their stoichiometry was ascertained by ^{1}H NMR spectroscopy. The bulk material appeared to be pure and homogeneous cocrystal composition by PXRD, which was

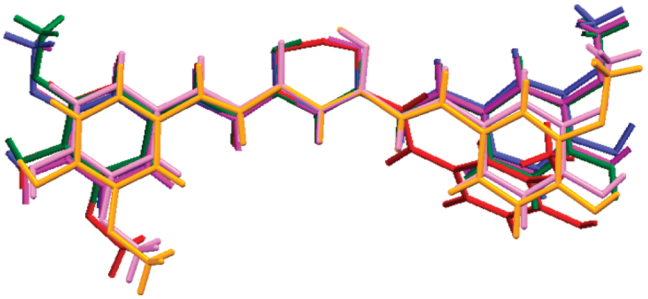

Figure 3. Molecular overlay of curcumin in form **1** (red), form **2** (blue, magenta), form **3** (green), curcumin−resorcinol cocrystal **1a** (light orange), and curcumin−pyrogallol cocrystal **1b** (pink). The two aryl side arms are nearly coplanar to the central β-keto−enol group in all crystal structures, except the stable commercial polymorph **1** of curcumin in which one styryl group is twisted.

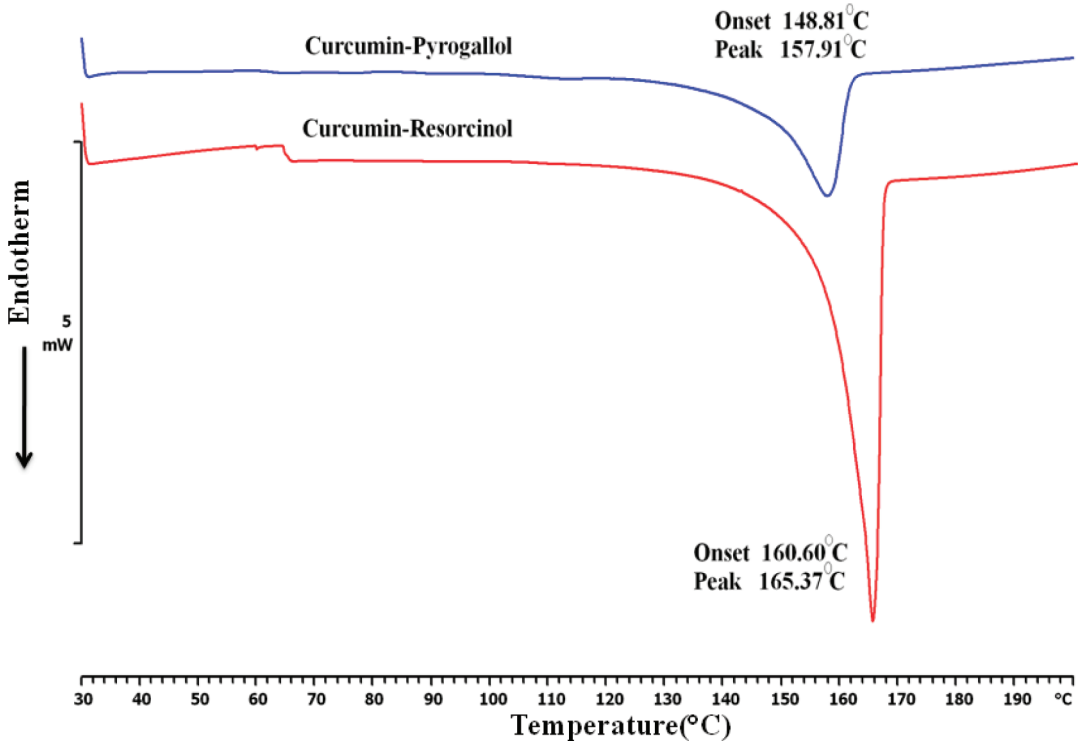

Figure 4. DSC endotherm of cocrystal **1a** and **1b**. The single endotherm at a temperature different from the melting points of the pure components is indicative of a homogeneous cocrystal phase. Melting point of curcumin is 177 °C, resorcinol, 110 °C, and pyrogallol, 131 °C.

Table 3. FT-IR Stretching Vibration Modes Wavenumber (ν_s, cm^{-1}) for Curcumin Cocrystals

	O−H	C═O	aromatic C═C	enol C−O	phenol C−O
curcumin	3510.9	1627.5	1602.6	1429.0	1281.2
curcumin−resorcinol	3439.7	1625.5	1603.3, 1593.2	1430.7	1283.8
curcumin−pyrogallol	3427.2 (br)	1626.6	1588.7	1429.6	1282.6
resorcinol	3257.3 (br)	–	1608.3	–	1297.3
pyrogallol	3527.4	–	1621.9	–	1285.3

confirmed by matching the experimental PXRD patterns with the calculated diffraction lines from the X-ray crystal structures (Supporting Information, Figure S2). The powder X-ray diffraction of curcumin−resorcinol (**1a**) exhibited characteristic reflections at about 2θ 10.91°, 18.81°, 20.12°, 23.39°, 24.05°, and 25.82 ± 0.2°. Curcumin−pyrogallol (**1b**) exhibited characteristic reflections at about 2θ 10.57°, 11.96°, 18.78°, 20.97°, 24.11°, 24.69°, and 26.66 ± 0.2°. Peak position (2θ), d spacing (Å), and intensity (%) are summarized in Table S1 (Supporting Information). Both cocrystals were found to be stable for up to 6 months in our laboratory ambient conditions of 25−35 °C and 40−60% relative humidity. A systematic check under ICH guidelines accelerated stability conditions of 40 °C and 75% RH in a controlled temperature−humidity chamber showed no sign of degradation or dissociation of cocrystals to curcumin at 3 months (13 weeks; see Table S2, Supporting Information).

FT-IR and FT-Raman and ss-NMR Spectroscopy. Infrared and Raman spectroscopy provide useful information about the vibrational modes of a molecule resulting from changes in the physical state of the sample and differences in hydrogen bonding and molecular conformations.[46] Hydroxyl groups absorb strongly in the 3700−3584 cm^{-1} region. Phenolic and olefinic C−O stretching vibrations occur between 1260 and 1000 and 1430−1410 cm^{-1}, respectively. IR spectra of cocrystals **1a** and **1b** alongside those of curcumin and the coformer are displayed in Figure S3 (Supporting Information). The changes in the O−H and C═O stretching frequencies of the cocrystals compared to the coformers suggested the formation of new compounds. Similarly, the Raman spectra exhibited diagnostic differences in the carbonyl stretch, phenol, and olefinic C−O stretch regions (Supporting Information, Figure S4). A comparison of IR and Raman stretching frequencies is summarized in Tables 3 and 4. Together with ss-NMR spectroscopy (discussed next), the formation of new cocrystals of curcumin was confirmed in the bulk phase.

Solid-state ^{13}C NMR spectroscopy[47,48] (ss-NMR) provides structural information about differences in hydrogen bonding, molecular conformation, molecular mobility, and short-range environment in crystalline and amorphous solids. The sharp peaks in the spectra of cocrystals **1a** and **1b** indicated their crystalline nature. Differences in the cocrystals of curcumin from the starting materials were analyzed by ^{13}C cross-polarization magic-angle spinning (CP-MAS) ss-NMR (Figure 5). The upfield chemical shift of the OMe carbon (δ ~55 ppm) and downfield shift movement of the carbonyl carbon atom of

dx.doi.org/10.1021/cg200704s |Cryst. Growth Des. 2011, 11, 4135–4145

Table 4. FT-Raman Stretching Vibration Modes Wavenumber (ν_s, cm^{-1}) for Curcumin Cocrystals

	C═O	aromatic C═C	enol C−O	phenol C−O
curcumin form **1**	1626.0	1600.3	1430.0	1249.3
curcumin−resorcinol	1639.0	1601.3	1426.2	1242.2
curcumin−pyrogallol	1627.0	1599.0	1429.5	1244.6
resorcinol	–	1606.4	1310.6	1084.6
pyrogallol	–	1624.9	1342.5	1156.7

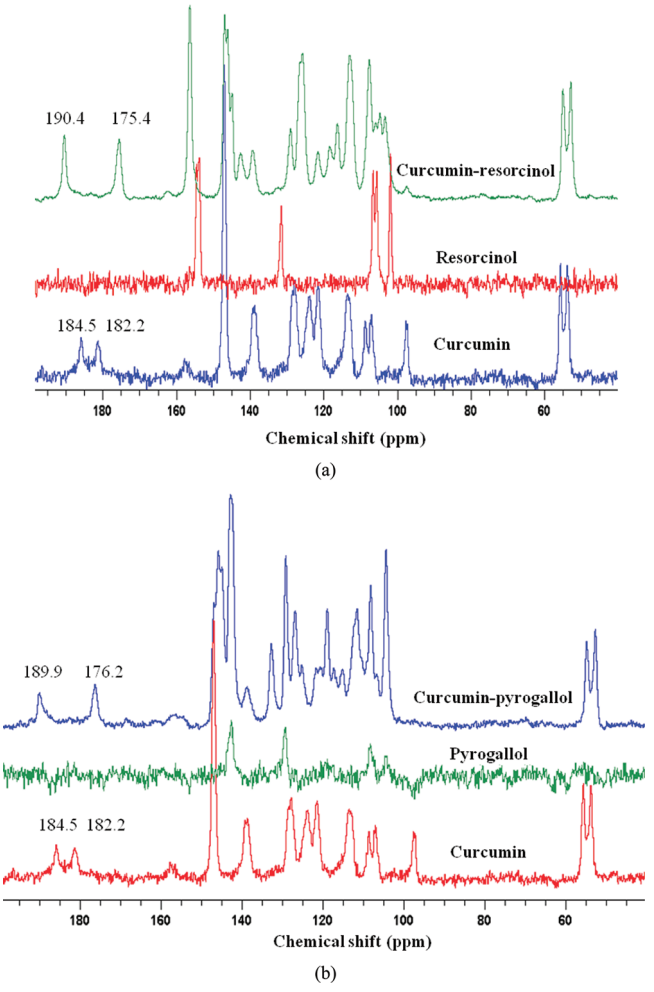

Figure 5. Solid state ^{13}C NMR spectra of (a) curcumin−resorcinol (**1a**) and (b) curcumin−pyrogallol (**1b**) cocrystals along with the pure components. The peaks in the cocrystal are shifted relative to the pure components.

curcumin (δ ~185 ppm) provided additional characterization of new solid materials **1a** and **1b**. The chemical shift values are summarized in Table S3 (Supporting Information).

Dissolution Experiments. The aqueous solubility of curcumin is very low (8.7 mg/L).[16] Its solubility is lower at acidic and neutral pH and higher under basic conditions. However, curcumin is unstable in the latter conditions; 90% of curcumin decomposes at pH 7.2 buffer within 30 min. Curcumin is soluble in EtOH and acetone and is stable in these media. The dissolution rate of curcumin polymorphs was determined in 40% EtOH−water medium in which it has higher solubility (stable form **1** = 1.21 g/L).

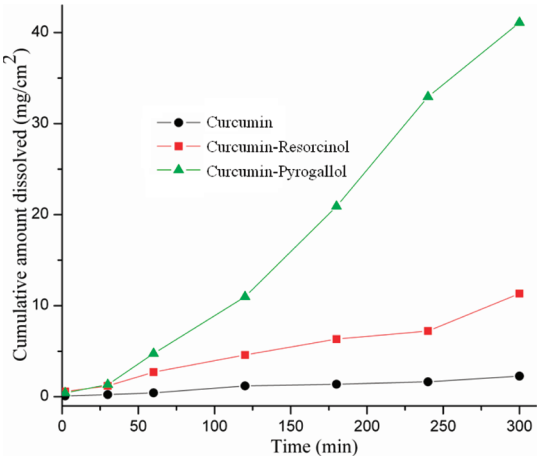

Figure 6. Intrinsic dissolution rate of curcumin form **1** (●), curcumin−resorcinol (■) and curcumin−pyrogallol (▲) in 40% EtOH−water at 37 °C. The amount of curcumin dissolved in solution was monitored by UV−vis spectroscopy.

The dissolution rate of form **2** is about 3 times faster than that of commercial form **1**.[26] The dissolution rates of curcumin cocrystals **1a** and **1b** were compared with that of the stable form **1** at 37 °C for 5 h. The intrinsic dissolution experiment could not be run beyond 5 h because at this time the pellet of cocrystal **1a** and **1b** started to disintegrate and a hole was observed in the center. The contact surface area of the pellet increased abruptly at this point, leading to faster dissolution of cocrystals and consequent supersaturation of curcumin released suddenly into the medium causing precipitation. In contrast, the pellet of pure curcumin was intact beyond 5 h. The amount of curcumin dissolved (mg/cm^2) was plotted against time (min) (Figure 6), and intrinsic dissolution rates were calculated (Table 5) from the slope in the linear region of the dissolution curves. Curcumin−pyrogallol (1:1) and curcumin−resorcinol (1:1) cocrystals dissolved ~12 and ~5 times faster than curcumin, respectively. The rate of dissolution and apparent solubility are different from equilibrium solubility. The former are kinetic parameters, while the latter is a thermodynamic quantity. Since most drugs exert their therapeutic effect within 4−6−8 h of oral administration, the apparent solubility of the drug is a relevant parameter for those solid-state drug forms that undergo phase transformation during the solubility experiment.

Solubility is defined as the concentration of the substance in solution that is at chemical equilibrium with an excess of the undissolved substance. The rate at which this equilibrium is reached is the dissolution rate. The solubility (after 24 h stirring, generally taken as an equilibrium value at 24−48 h) of curcumin form **1**, cocrystal **1a**, and cocrystal **1b** are 1.21, 2.02, and 5.97 g/L, respectively (curcumin form **2** = 2.12 g/L).[26] However, both cocrystals **1a** and **1b** were not indefinitely stable in the slurry medium of the dissolution experiment and converted to stable form **1** of curcumin as concluded from their PXRD plots (see Figures S5 and S6, Supporting Information). When the solid form is not stable during the solubility experiment, as in the present case, the apparent solubility[49,50] may be calculated for comparison. The apparent solubility is the rate at which the cocrystal dissolves with respect to the stable form, multiplied by the solubility of the stable form (eq 1).

$$C_m = C_s(J_m/J_s) \quad (1)$$

dx.doi.org/10.1021/cg200704s |*Cryst. Growth Des.* 2011, 11, 4135–4145

Table 5. Dissolution and Solubility Data for Curcumin Polymorphs and Cocrystals 1a and 1b. [a]

curcumin forms	absorption coefficient (ε), (mM^{-1} cm^{-1})	solubility at 37 °C (24 h) in 40% ethanol−water (g/L)	intrinsic dissolution rate ($\times10^{-3}$) (mg/cm^2)/min	apparent solubility[b] (g/L)
curcumin polymorph **1**	46.21	1.21	7.96	1.21
curcumin−resorcinol (**1a**)	37.15	2.02 (×1.67)	37.61 (×4.72)	5.71
curcumin−pyrogallol (**1b**)	52.42	5.97 (×4.93)	93.64 (×11.76)	14.23
curcumin polymorph **2**	43.99	2.12 (×1.75)	25.26 (×3.17)	3.84

[a] The extent of increase (×) relative to curcumin polymorph **1** is given in parentheses. [b] Calculated using eq 1, given in text.

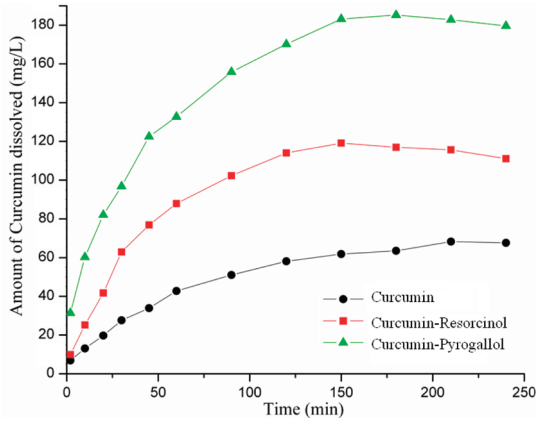

Figure 7. Powder dissolution curves for curcumin form **1** (●), cocrystal **1a** (■), and cocrystal **1b** (▲) in 40% EtOH−water at 37 °C. The curcumin concentration for cocrystals reaches a peak value at about 2.5 h and then starts to decrease slowly because of transformation to the stable polymorph **1** in the slurry medium.

where C_m is the apparent solubility of the cocrystal, C_s is the solubility of the thermodynamic form, and J_m and J_s are the dissolution rates for the cocrystal and the stable species (derived from the linear region of the drug concentration vs time plots). The apparent solubilities of curcumin−resorcinol (**1a**) and curcumin−pyrogallol (**1b**) cocrystals are 5.71 and 14.23 g/L, respectively (curcumin form **2** = 3.84 g/L). Powder dissolution experiments (Figure 7) were carried out on materials sieved to ∼200 μm particle size. Peak solubilities were achieved at 2.5 h (form **1** = 60 mg/L, **1a** = 118 mg/L, **1b** = 182 mg/L), and then steady-state plateau concentrations were maintained until 4 h. The amount of curcumin dissolved in 4 h ($AUC_{0-4\,h}$) of powder dissolution in 40% EtOH−water (see Table S4 for AUC calculations, Supporting Information) is 12.2 g h/L for form **1**, 23.3 g h/L for cocrystal **1a**, and 36.5 g h/L for cocrystal **1b**. The fact that both curcumin−pyrogallol and curcumin−resorcinol are stable in the early phase of the dissolution experiment (up to 2−4 h) (verified by placing 200 mg of cocrystal in 5 mL of 40% EtOH−water mixture) is an encouraging result (Figure 8). There was no trace of curcumin by PXRD after 2 h, but the cocrystals transformed to curcumin after 4 h (Figure S7, Supporting Information). In contrast, the faster dissolving polymorph **2** of curcumin transformed to the stable modification in less than 1 h.

The higher apparent solubility of curcumin cocrystals **1a** and **1b** compared to the metastable polymorph **2** is consistent with the general trend for polymorphs and cocrystals. Solubility improvement among crystalline drug polymorphs is about 2−3 times,[51] with the less stable polymorph being more soluble. Cocrystal solubility can often match with that of the amorphous drug,[5,6,44] and these latter values are much higher (4−14-fold)[52] than that of the crystalline form. We noted the inverse correlation between melting point and solubility: the higher melting curcumin−resorcinol (**1a**) has lower solubility than the lower melting curcumin−pyrogallol cocrystal (**1b**). The data in Table 5 suggest that cocrystals **1a** and **1b** have a greater potential in solid form development for curcumin compared to the metastable polymorph because of their faster dissolution performance and improved stability. The concentration of curcumin in dissolution and solubility experiments was assayed spectrophotometrically at the 430 nm maxima from standardized concentration−intensity UV−vis plots; there was no interference from coformers that absorb in the blue-shifted 250−270 nm UV region. We noted a structural similarity among the more soluble forms: the curcumin molecule is near-planar in the metastable polymorph **2** and cocrystals **1a** and **1b**, whereas it is bent in the stable polymorph. A possible explanation could be that the extended planarity[53] and conjugation of curcumin molecule are responsible for increased solubility. Conjugation is more effective in the planar structures because they are bright red colored compared to the deep yellow color of commercial curcumin. Another speculation is that that the more soluble coformer makes O−H···O hydrogen bonds with water and thereby facilitates release of curcumin from the cocrystal into the aqueous medium.

■ CONCLUSIONS

A major problem in the use of bioactive herbal ingredient curcumin as a therapeutic agent is its low solubility and bioavailability. The present results on more soluble cocrystals of curcumin could provide faster dissolving solid forms of curcumin that are relatively stable for drug development. These results are of general applicability in that cocrystals could offer the dual advantage of higher solubility and improved stability compared to fast dissolving polymorphs, which are often metastable. A crystal engineering approach was utilized to prepare 1:1 cocrystals of curcumin with resorcinol and pyrogallol by liquid-assisted grinding. The products **1a** and **1b** were characterized by IR, Raman, ss-NMR, and X-ray diffraction. These are the earliest examples of curcumin cocrystals with complete structural characterization and physicochemical measurements to our knowledge. Pending in vivo clinical data, we believe that the faster dissolving curcumin cocrystals hint at improved bioavailability than pure curcumin.

■ EXPERIMENTAL SECTION

Curcumin was purchased from Sigma-Aldrich (Hyderabad, Andhra Pradesh, India) and used directly for experiments. All other chemicals were of analytical or chromatographic grade. Melting points were measured on a Fisher-Johns melting point apparatus. Water filtered

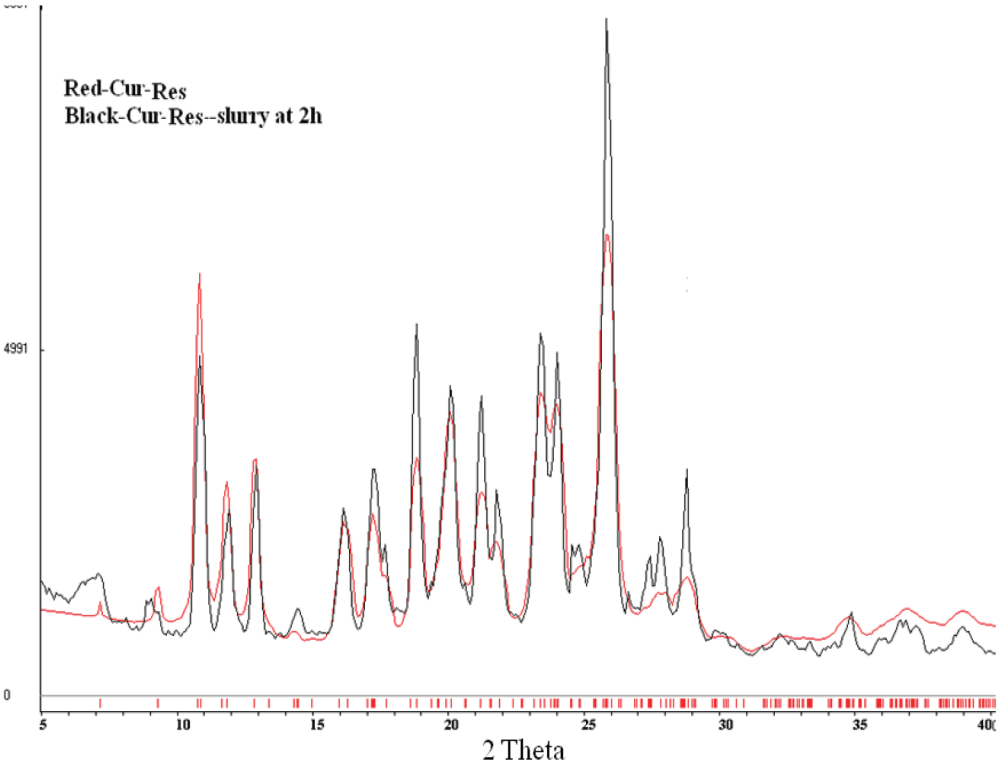

(a)

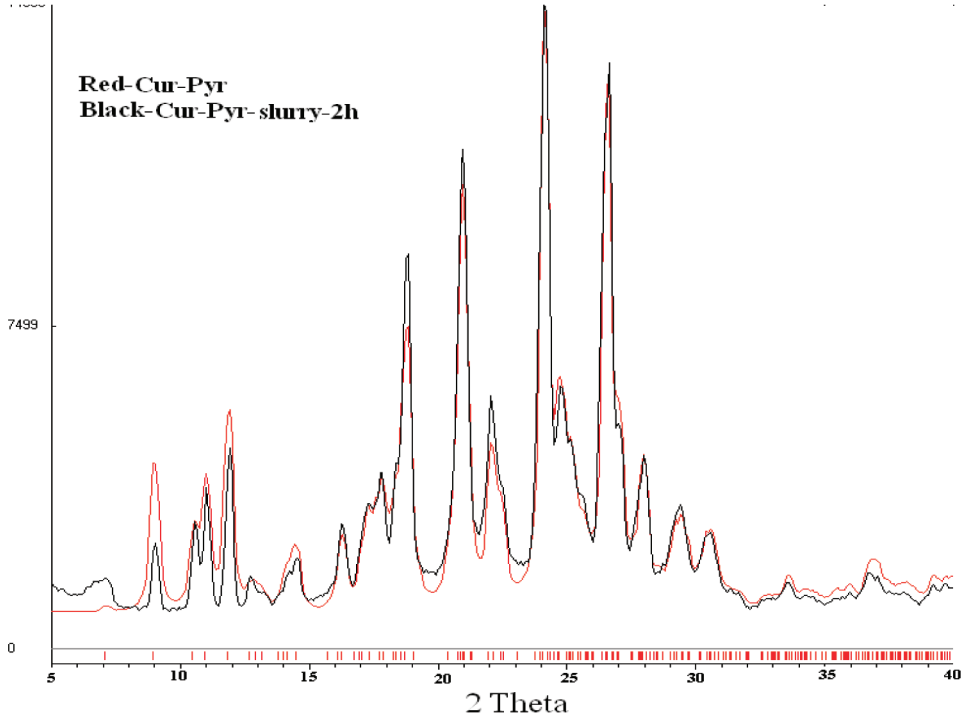

(b)

Figure 8. PXRD of curcumin−resorcinol (a) and curcumin−pyrogallol (b) cocrystals (black line experimental) after slurry for 2 h overlay on the calculated lines from the X-ray crystal structure (red). The cocrystals are stable for up to 2 h in 40% EtOH−water medium.

Table 6. Crystallization Conditions for Curcumin Cocrystals

cocrystal	condition	time (d)
curcumin−resorcinol (1:1), **1a**	(a) solution crystallization for single crystals: 200 mg (0.54 mmol) of curcumin and 59.5 mg (0.54 mmol) of resorcinol were ground in a mortar−pestle for 30 min after adding 5 drops of EtOH and then kept for crystallization in EtOH−benzene mixture (18 mL + 2 mL) (b) liquid-assisted grinding method for bulk material: 200 mg (0.54 mmol) of curcumin and 59.5 mg (0.54 mmol) of resorcinol were ground in a mortar−pestle for 30 min after adding of 5−6 drops of EtOH, which gave the cocrystal as a microcrystalline powder	3−4
Curcumin−pyrogallol (1:1), **1b**	(a) solution crystallization for single crystals: 200 mg (0.54 mmol) of curcumin and 68.1 mg (0.54 mmol) of pyrogallol were ground in a mortar−pestle for 30 min after adding 5 drops of EtOH and then kept for crystallization in EtOH−benzene mixture (18 mL + 2 mL) (b) liquid-assisted grinding method for bulk material: 200 mg (0.54 mmol) of curcumin and 68.1 mg (0.54 mmol) of pyrogallol were ground in a mortar−pestle for 30 min after adding 5−6 drops of EtOH to give the cocrystal as a microcrystalline powder	3−4

through a double deionized purification system (Milli Q Plus Water System; Millipore Co., Billeria, MA) was used in all the experiments.

Crystallization. The procedures for preparing microcrystalline powders (bulk material for measurements) and single crystals (for X-ray diffraction) of products are detailed in Table 6. The use of EtOH in liquid-assisted grinding did not show any apparent evidence of ethanol solvates as judged from the ^{1}H NMR spectra of products that were devoid of solvent peaks. Liquid-assisted grinding followed by solution crystallization gave single crystals, but the first stage was not mandatory; an equimolar mixture of components in solution crystallization gave similar results.

Single Crystal X-ray Diffraction. A single crystal obtained from the crystallization solvent(s) given in Table 6 was mounted on the goniometer of an Oxford CCD X-ray diffractometer (Yarnton, Oxford, UK) equipped with a Mo Kα radiation (λ = 0.710 73 Å) source. Data reduction was performed using CrysAlisPro 171.33.55 software.[54] Crystal structures were solved and refined using Olex2-1.0[55] with anisotropic displacement parameters for non-H atoms. Hydrogens on O atoms were experimentally located through the Fourier difference electron density maps in all crystal structures. All O−H and C−H atoms were geometrically fixed using HFIX, DFIX, DANG, and FLAT command in SHELX-TL program of Bruker-AXS.[56] A check of the final .cif file with PLATON[57] did not show any missed symmetry. X-ray data of curcumin−resorcinol (**1a**) and curcumin−pyrogallol (**1b**) were collected at 298 and 100 K to get the lowest *R*-factor with the best crystallographic parameters. The quality of single crystals was not of the best transparency for X-ray diffraction (because they were thin and fragile) but the best quality that we were able to obtain for data collection. X-Seed[58] was used to prepare the crystal structures figures and packing diagrams. Crystallographic parameters of both structures are summarized in Table 1. Hydrogen-bond distances in Table 2 are neutron-normalized to fix the D−H distance to its accurate neutron value in the X-ray crystal structures (O−H 0.983 Å, C−H 1.083 Å). Crystallographic .cif files (CCDC Nos. 825957 and 825958) are available at www.ccdc.cam.ac.uk/data_request/cif or as part of the Supporting Information.

Powder X-ray Diffraction. PXRD were recorded on a SMART Bruker D8 Advance X-ray diffractometer (Bruker-AXS, Karlsruhe, Germany) using Cu Kα X-radiation (λ = 1.5406 Å) at 40 kV and 30 mA. Diffraction patterns were collected over the 2θ range of 5−50° at a scan rate of 1°/min. The formation of cocrystal was monitored by the appearance of new diffraction lines. Powder Cell 2.3[59] was used for overlaying the experimental PXRD pattern on the calculated lines from the crystal structure.

Thermal Analysis. DSC was performed on a Mettler Toledo DSC 822e module (Columbus, OH). A 4−6 mg portion of the sample was placed in crimped but vented aluminum pans and the temperature range was 30−200 °C at heating rate of 5 °C min^{-1}. The sample was purged by a stream of dry nitrogen flowing at 80 mL min^{-1}.

Vibrational Spectroscopy. A Thermo-Nicolet 6700 FT-IR spectrometer (Waltham, MA) with a NXR FT-Raman module (Nd:YAG laser source, 1064 nm wavelength) was used to record IR and Raman spectra. IR spectra were recorded on samples dispersed in KBr pellets. Raman spectra were recorded on samples contained in standard NMR diameter tubes or on compressed samples contained in a gold-coated sample holder.

Solid-State NMR Spectroscopy. Solid-state ^{13}C NMR (ss-NMR) spectroscopy provides structural information about differences in hydrogen bonding, molecular conformations, and molecular mobility in the solid state. The solid-state ^{13}C NMR spectra were obtained on a Bruker Ultrashield 400 spectrometer (Bruker BioSpin, Karlsruhe, Germany) utilizing a ^{13}C resonant frequency of 100 MHz (magnetic field strength of 9.39 T). Approximately 100 mg of sample was lightly packed into a zirconium rotor with a Kel-F cap. The cross-polarization magic angle spinning (CP-MAS) pulse sequence was used for spectral acquisition. Each sample was spun at a frequency of 5.0 ± 0.01 kHz and the magic angle setting calibrated by the KBr method. Each data set was subjected to a 5.0 Hz line broadening factor and subsequently Fourier-transformed and phase-corrected to produce a frequency domain spectrum. The chemical shifts were referenced to TMS using glycine ($\delta_{glycine}$ = 43.3 ppm) as an external secondary standard.

Dissolution and Solubility Experiments. Intrinsic dissolution rate (IDR) and solubility measurements were carried out on a USP-certified Electrolab TDT-08 L dissolution tester (Electrolab, Mumbai, MH, India). A calibration curve was obtained for curcumin form **1** and cocrystals **1a** and **1b** by plotting absorbance vs concentration UV−vis spectra curves on a Thermo Scientific Evolution EV300 UV−vis spectrometer (Waltham, MA) for known concentration solutions in 40% EtOH−water medium. The mixed solvent system (EtOH−water) was selected for its higher solubility of curcumin in this medium. The slope of the plot from the standard curve gave the molar extinction coefficient (ε) by applying Beer−Lambert's law. Equilibrium solubility was determined in 40% EtOH−water medium using the shake-flask method.[60] To obtain the equilibrium solubility, 100 mg of each solid material was stirred for 24 h in 5 mL of 40% EtOH−water at 37 °C, and the absorbance was measured at 430 nm. The concentration of the saturated solution was calculated at 24 h, which is referred to as the equilibrium solubility of the stable solid form (C_s). The apparent solubility (C_m) is more appropriate for cocrystals **1a** and **1b**, because they were found to transform to the stable form **1** of curcumin under the solubility measurement conditions. The apparent solubility (C_m) of a cocrystal is calculated using eq 1. The dissolution rates J_s and J_m are obtained from the IDR experiments.

A 100 mg portion of the solid (drug, cocrystal, polymorph) was taken in the intrinsic attachment and compressed to a 0.5 cm^2 pellet using a hydraulic press at a pressure of 2.5 ton/$in.^2$ for 2 min. The pellet was compressed to provide a flat surface on one side and the other side was sealed. Then the pellet was dipped into 900 mL of 40% EtOH−water medium at 37 °C with the paddle rotating at 150 rpm. At regular intervals of 10 min, 5 mL of the dissolution medium was withdrawn and replaced by an equal volume of fresh medium to maintain a constant volume. Samples were filtered through 0.2 μm nylon filter and assayed for drug content spectrophotometrically at 430 nm on a Thermo-Nicolet EV300 UV−vis spectrometer. There was no interference to the curcumin UV−vis maxima at 430 nm by the coformers, because resorcinol and pyrogallol absorb at 250−270 nm in the UV region. The amount of drug dissolved in each time interval was calculated using the calibration curve. The linear region of the dissolution profile was used to determine the intrinsic dissolution rate (IDR) of the compound [=slope of the curve, i.e., amount of drug dissolved divided by the surface area of the disk (0.5 cm^2) per minute]. The dissolution rates for form **1** and cocrystals **1a** and **1b** of curcumin were computed from their IDR values.

For powder dissolution studies of curcumin and its cocrystals, the starting solids were sieved in ASTM standard mesh sieves to provide samples with particle size of approximately 200 μm and then directly poured into 900 mL of dissolution medium, and the paddle rotation was fixed at 100 rpm. Dissolution experiments were continued up to 4 h at 37 °C. At regular intervals of 5−10 min, 5 mL of the dissolution medium was drawn and replaced by an equal volume of fresh medium to maintain a constant volume. The area under the curve for 4 h of dissolution experiment (AUC_{0-4h}) was calculated by the linear trapezoidal rule of drug bioavailability.[61]

■ ASSOCIATED CONTENT

Supporting Information. Powder X-ray diffraction values, ORTEP diagrams, ss-NMR chemical shifts, PXRD plots after solubility experiments, crystallographic .cif files, and PLATON check reports. This material is available free of charge via the Internet at http://pubs.acs.org.

■ AUTHOR INFORMATION

Corresponding Author

*E-mail: ashwini.nangia@gmail.com.

■ ACKNOWLEDGMENT

We thank the DST for research funding (SR/S1/OC-67/2006), JC Bose fellowship (SR/S2/JCB-06/2009), and CSIR grant (01(2410)/10/EMR-II) and DST (IRPHA) and UGC (PURSE grant) for providing instrumentation and infrastructure facilities. P.S., N.R.G., and U.B.R.K. thank the UGC, CSIR, and Crystalin Research for fellowship.

■ REFERENCES

(1) Kola, I.; Landis, J. Can the pharmaceutical industry reduce attrition rates? *Nat. Rev. Drug Discovery* **2004**, *3*, 711–715.

(2) Stahly, G. P. A Survey of cocrystals reported prior to 2000. *Cryst. Growth Des.* **2009**, *9*, 4212–4229.

(3) Vishweshwar, P.; McMahon, J. A.; Bis, J. A.; Zaworotko, M. J. Pharmaceutical co-crystals (review). *J. Pharm. Sci.* **2006**, *95*, 499–516.

(4) US Food and Drug administration approved GRAS list. EAFUS: A food additive database. http://www.cfsan.fda.gov/_dms/ eafus.html.

(5) Remenar, J. F.; Morissette, S. L.; Peterson, M. L.; Moulton, B.; MacPhee, J. M.; Guzmán, H. R.; Almarsson, Ö. Crystal engineering of novel co-crystals of a triazole drug with 1,4-dicarboxylic acids. *J. Am. Chem. Soc.* **2003**, *125*, 8456–8457.

(6) Babu, N. J.; Nangia, A. Solubility advantage of amorphous drugs and pharmaceutical cocrystals. *Cryst. Growth Des.* **2011**, *11*, 2662–2679.

(7) Amidon, G. L.; Lennernas, H.; Shah, V. P.; Crison, J. R. Theoretical basis for a biopharmaceutical drug classification: Correlation of in vitro drug product dissolution and in vivo bioavailability. *Pharm. Res.* **1995**, *12*, 413–420.

(8) Çıkrıkçı, S.; Mozioğlu, E.; Yılmaz, H. Biological activity of curcuminoids isolated from curcuma longa. *Rec. Nat. Prod.* **2008**, *2*, 19–24.

(9) Hatcher, H.; Planalp, R.; Cho, J.; Torti, F. M.; Torti, S. V. Curcumin: From ancient medicine to current clinical trials (review). *Cell. Mol. Life Sci.* **2008**, *65*, 1631–1652.

(10) Mahady, G. B.; Pendland, S. L.; Yun, G; Lu, Z. Z. Turmeric (*Curcuma longa*) and curcumin inhibit the growth of *Helicobacter pylori*, a group 1 carcinogen. *Anticancer Res.* **2002**, *22*, 4179–4181.

(11) Sugiyama, Y.; Kawakishi, S.; Osawa, T. Involvement of the beta-diketone moiety in the antioxidative mechanism of tetrahydrocurcumin. *Biochem. Pharmacol.* **1996**, *52*, 519–525.

(12) Ruby, A. J.; Kuttan, G.; Babu, K. D.; Rajasekharan, K. N.; Kuttan, R. Anti-tumour and antioxidant activity of natural curcuminoids. *Cancer Lett.* **1995**, *94*, 79–83.

(13) Jordan, W. C.; Drew, C. R. Curcumin—A natural herb with anti-HIV activity. *J. Natl. Med. Assoc.* **1996**, *88*, 333–335.

(14) Qureshi, S.; Shah, A. H.; Ageel, A. M. Toxicity studies on *Alpinia alangal* and *Curcuma longa*. *Planta Med.* **1992**, *58*, 124–127.

(15) Lao, C. D.; Ruffin, M. T.; Normolle, D.; Heath, D. D.; Murray, S. I.; Bailey, J. M.; Boggs, M. E.; Crowell, J.; Rock, C. L.; Brenner, D. E. Dose escalation of a curcuminoid formulation. *BMC Complement, Altern. Med.* **2006**, *6*, 10.

(16) Anand, P.; Kunnumakkara, A. B.; Newman, R. A.; Aggarwal, B. B. Bioavailability of curcumin: Problems and promises (review). *Mol. Pharmaceutics* **2007**, *4*, 807–818.

(17) Wang, Y. J.; Pan, M. H.; Cheng, A. L.; Lin, L. I.; Ho, Y. S.; Hsieh, C. Y.; Lin, J. K. Stability of curcumin in buffer solutions and characterization of its degradation products. *J. Pharm. Biomed. Anal.* **1997**, *15*, 1867–1876.

(18) Antony, B.; Merina, B.; Iyer, V. S.; Judy, N.; Lennertz, K.; Joyal, S. A. Pilot cross-over study to evaluate human oral bioavailability of BCM-95 CG (Biocurcumax) a novel bioenhanced preparation of curcumin. *Ind. J. Pharm. Sci.* **2008**, 445–449.

(19) Zhang, F.; Koh, G. K.; Jeansonne, D. P.; Hollingworth, J.; Russo, P. S.; Vicente, G.; Stout, R. W.; Liu, Z. A Novel solubility-enhanced curcumin formulation showing stability and maintenance of anticancer activity. *J. Pharm. Sci.* **2011**, *100*, 2778–2789.

(20) Gupta, N. K.; Dixit, V. K. Bioavailability enhancement of curcumin by complexation with phosphatidyl choline. *J. Pharm. Sci.* **2011**, *100*, 1987–1995.

(21) Schultheiss, N.; Bethune, S.; Henck, J.-O. Nutraceutical cocrystals: Utilizing pterostilbene as a cocrystal former. *CrystEngComm* **2010**, *12*, 2436–2442.

(22) Karki, S.; Friščić, T.; Fábián, L.; Jones, W. New solid forms of artemisinin obtained through cocrystallisation. *CrystEngComm* **2010**, *12*, 4038–4041.

(23) Bethune, S. J.; Schultheiss, N.; Henck, J.-O. Improving the poor aqueous solubility of nutraceutical compound pterostilbene through cocrystal formation. *Cryst. Growth Des.* **2011**, *11*, 2817–2823.

(24) Schultheiss, N.; Newman, A. Pharmaceutical cocrystals and their physicochemical properties. *Cryst. Growth Des.* **2009**, *9*, 2950–2967.

(25) McNamara, D. P.; Childs, S. L.; Giordano, J.; Iarriccio, A.; Cassidy, J.; Shet, M. S.; Mannion, R.; O'Donnell, E.; Park, A. Use of a glutaric acid cocrystal to improve oral bioavailability of a low solubility API. *Pharm. Res.* **2006**, *23*, 1888–1897.

(26) Sanphui, P.; Goud, N. R.; Khandavilli, U. B. R.; Bhanoth., S.; Nangia, A. Novel polymorphs of curcumin. *Chem. Commun.* **2011**, *47*, 5013–5015.

(27) Mukherjee, A.; Grobelny, P.; Thakur, T. S.; Desiraju, G. R. Polymorphs, pseudopolymorphs and co-crystals of orcinol: Exploring

the structural landscape through high throughput crystallography. *Cryst. Growth Des.* **2011**, *11*, 2637–2653.
(28) Yang, C. J.; Wang, C. S.; Hung, J. Y.; Huang, H. W.; Chia, Y. C.; Wang, P. H.; Weng, C. F.; Huang, M. S. Pyrogallol induces G2-M arrest in human lung cancer cells and inhibits tumor growth in an animal model. *Lung Cancer* **2009**, *66*, 162–168.
(29) Tang, G.; Yang, C. Y.; Nikolovska-Coleska, Z.; Guo, J.; Qiu, S.; Wang, R.; Gao, W.; Wang, G.; Stuckey, J.; Krajewski, K.; Jiang, S.; Roller, P. P.; Wang, S. Pyrogallol based molecules as potent inhibitors of the anti-apoptotic Bcl-2 proteins. *J. Med. Chem.* **2007**, *50*, 1723–1726.
(30) Trask, A. V.; Motherwell, W. D. S.; Jones, W. Solvent-drop grinding: Green polymorph control of cocrystallisation. *Chem. Commun.* **2004**, 890–891.
(31) Balasubramanian, K. Molecular orbital basis for yellow curry spice curcumin's prevention of Alzheimer's disease. *J. Agric. Food Chem.* **2006**, *54*, 3512–3520.
(32) Parimita, S. P.; Ramshankar, Y. V.; Suresh, S.; Row, T. N. G. Redetermination of curcumin: (1*E*,4*Z*,6*E*)-5-Hydroxy-1,7-bis(4-hydroxy-3-methoxyphenyl)hepta-1,4,6-trien-3-one. *Acta Crystallogr.* **2007**, *E63*, o860–o862.
(33) Bernstein, J.; Davis, R. E.; Shimoni, L.; Chang, N.-L. Patterns in hydrogen bonding: Functionality and graph set analysis in crystals. *Angew. Chem., Int. Ed. Engl.* **1995**, *34*, 1555–1573.
(34) Cambridge Structural Database, Ver. 5.32, May 2011 update, Cambridge Crystallographic Data Center, UK; www.ccdc.cam.ac.uk.
(35) Ermer, O.; Robke, C. Crystal Structure of 2,5-di-*tert*-butylhydroquinone: Polar stacking of nonpolar hydrogen-bonded sheets with trigonal symmetry. *Angew. Chem., Int. Ed. Engl.* **1994**, *33*, 1755−1757. [Refcode HESKOF]
(36) Dinger, M. B.; Scott, M. J. Extended structures built on a triphenoxymethane platform. C3-symmetric, conformational mimics of calix[*n*]arenes. *Eur. J. Org. Chem.* **2000**, 2467−2478. [Refcode QEXXEW]
(37) Parvez, M.; Kurtz, S. K.; Williams, I. Structure of a melanin precursor: 1-Methylindole-5,6-diol. *Acta Crystallogr.* **1990**, *C46*, 165−167. [Refcode SEFRIE]
(38) Andresen, T. L.; Krebs, F. C.; Thorup, N.; Bechgaard, K. Crystal Structures of 2,3,6,7,10,11-oxytriphenylenes. Implications for columnar discotic mesophases. *Chem. Mater.* **2000**, *12*, 2428−2433. [Refcode XEFSIK]
(39) Ma, Z.; Moulton, B. Supramolecular medicinal chemistry: Mixed-ligand medicinal chemistry. *Mol. Pharmaceutics* **2007**, *4*, 373–385.
(40) Aitipamula, S.; Chowa, P. S.; Tan, R. B. H. Trimorphs of a pharmaceutical cocrystal involving two active pharmaceutical ingredients: Potential relevance to combination drugs. *CrystEngComm* **2009**, *11*, 1823–1827.
(41) Bhatt, P. M.; Azim, Y.; Thakur, T. S.; Desiraju, G. R. Co-crystals of the anti-HIV drugs lamivudine and zidovudine. *Cryst. Growth Des.* **2009**, *9*, 951–957.
(42) Stanton, M. K.; Tufekcic, S.; Morgan, C.; Bak, A. Drug substance and former structure−property relationships in 15 diverse pharmaceutical co-crystals. *Cryst. Growth Des.* **2009**, *9*, 1344–1352.
(43) Thakuria, R.; Nangia, A. Highly soluble olanzapinium maleate crystalline salts. *CrystEngComm.* **2011**, *13*, 1759–1764.
(44) Remenar, J. F.; Peterson, M. L.; Stephens, P. W.; Zhang, Z.; Zimenkov, Y.; Hickey, M. B. Celecoxib:nicotinamide dissociation: Using excipients to capture the cocrystal's potential. *Mol. Pharmaceutics* **2007**, *4*, 386–400.
(45) Li, J.; Bourne, S. A.; Caira, M. R. New polymorphs of nicotinamide and isonicotinamide. *Chem. Commun.* **2011**, *47*, 1530–1532.
(46) Elbagerma, M. A.; Edwards, H. G. M.; Munshi, T.; Hargreaves, M. D.; Matousek, P.; Scowen, I. J. Characterization of new cocrystals by Raman spectroscopy, powder X-ray diffraction, differential scanning calorimetry, and transmission Raman spectroscopy. *Cryst. Growth Des.* **2010**, *10*, 2360–2371.
(47) Tishmack, P. A.; Bugay, D. E.; Byrn, S. R. Solid-state nuclear magnetic resonance spectroscopy—Pharmaceutical applications (mini review). *J. Pharm. Sci.* **2002**, *92*, 441–474.
(48) Vogt, F. G.; Clawson, J. S.; Strohmeier, M.; Edwards, A. J.; Pham, T. N.; Watson, S. A. Solid-state NMR analysis of organic cocrystals and complexes. *Cryst. Growth Des.* **2009**, *9*, 921–937.
(49) Fagerberg, J. H.; Tsinman, O.; Sun, N.; Tsinman, K.; Avdeef, A.; Bergström, C. A. S. Dissolution rate and apparent solubility of poorly soluble drugs in biorelevant dissolution media. *Mol. Pharmaceutics* **2010**, *7*, 1419–1430.
(50) Otsuka, M.; Teraoka, R.; Matsuda, Y. Physicochemical properties of nitrofurantoin anhydrate and monohydrate and their dissolution. *Chem. Pharm. Bull.* **1991**, *39*, 2667–2671.
(51) Pudipeddi, M.; Serajuddin, A. T. M. Trends in solubility of polymorphs. *J. Pharm. Sci.* **2005**, *94*, 929–939.
(52) Hancock, B. C.; Parks, M. What is the true solubility advantage of amorphous pharmaceuticals? *Pharm. Res.* **2000**, *17*, 397–404.
(53) Murashima, T.; Tsujimoto, S.; Yamada, T.; Miyazawa, T.; Uno, H.; Ono, N.; Sugimoto, N. Synthesis of water-soluble porphyrin and the corresponding highly planar benzoporphyrin without meso-substituents. *Tetrahedron Lett.* **2005**, *46*, 113–116.
(54) *CrysAlis CCD and CrysAlis RED, versions 1.171.33.55*; Oxford Diffraction Ltd, Yarnton, Oxfordshire, UK, 2008
(55) Dolomanov, O. V.; Bourhis, L. J.; Gildea, R. J.; Howard, J. A. K.; Puschmann, H. OLEX2: A complete structure solution, refinement and analysis program. *J. Appl. Crystallogr.* **2009**, *42*, 339–341.
(56) *SMART, version 5.625 and SHELX-TL, version 6.12*; Bruker AXS Inc., Madison, WI, 2000.
(57) Spek, A. L. *PLATON, A Multipurpose Crystallographic Tool*; Utrecht University, Utrecht, Netherlands, 2002. Spek, A. L. Single-crystal structure validation with the program PLATON. *J. Appl. Crystallogr.* **2003**, *36*, 7–13.
(58) Barbour, L. J. *X-Seed, Graphical Interface to SHELX-97 and POV-Ray, a Program for Better Quality of Crystallographic Figures*; 1999. University of Missouri-Columbia, Missouri.
(59) Kraus, N.; Nolze, G. *Powder Cell, Version 2.3. A Program for Structure Visualization, Powder Pattern Calculation and Profile Fitting*; Federal Institute for Materials Research and Testing: Berlin, 2000.
(60) Glomme, A.; Marz, J.; Dressman, J. B. Comparison of miniaturized shake-flask solubility method with automated potentiometric acid/base titration and calculated solubilities. *J. Pharm. Sci.* **2005**, *94*, 1–16.
(61) Viscomi, G. C.; Campana, M.; Barbanti, M.; Grepioni, F.; Polito, M.; Confortini, D.; Rosini, G.; Righi, P.; Cannata, V.; Braga, D. Crystal forms of rifaximin and their effect on pharmaceutical properties. *CrystEngComm* **2008**, *10*, 1074–1081.